SUPPLEMENTARY INFORMATION

# Nano-engineered Electron-Hole Exchange Interaction Controls Exciton Dynamics in Core-Shell Semiconductor Nanocrystals

S. Brovelli, R.D. Schaller, S.A. Crooker, F. Garcia-Santamaria, Y. Chen, R. Viswanatha, J. A. Hollingsworth, H. Htoon, and V. I. Klimov

## Supplementary Figures

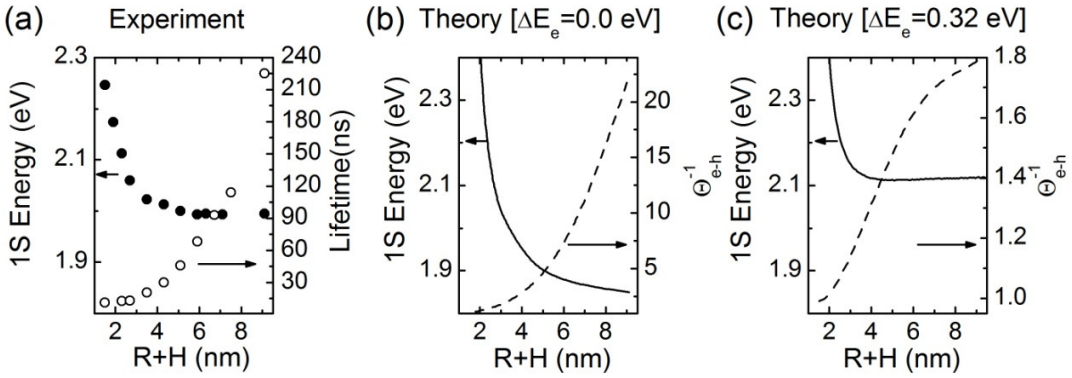


**Supplementary Figure S1. Effects of increasing shell thickness on the 1S transition energy and exciton recombination dynamics: Experiment and theoretical modeling** (a) Experimental measurements of the PL spectral energy for CdSe/CdS NCs as a function of the total particle radius, $R + H$ (solid circles). The PL lifetimes for diluted hexane solutions excited at 400 nm (peak power ~$2\times10^{15}$ photons · $pulse^{-1}$ · $cm^{-2}$) are reported as open circles. Calculations of the energy of the 1S transition (solid line) and the inverse of the electron-hole overlap integral (dashed line) for CdSe/*x*CdS NCs with increasing shell thickness using different values for the conduction-band energy offset at the CdSe/CdS interface: (b) $\Delta E_e = 0$ eV and (c) $\Delta E_e = 0.32$ eV. All NCs have the same core radius $R = 1.5$ nm.

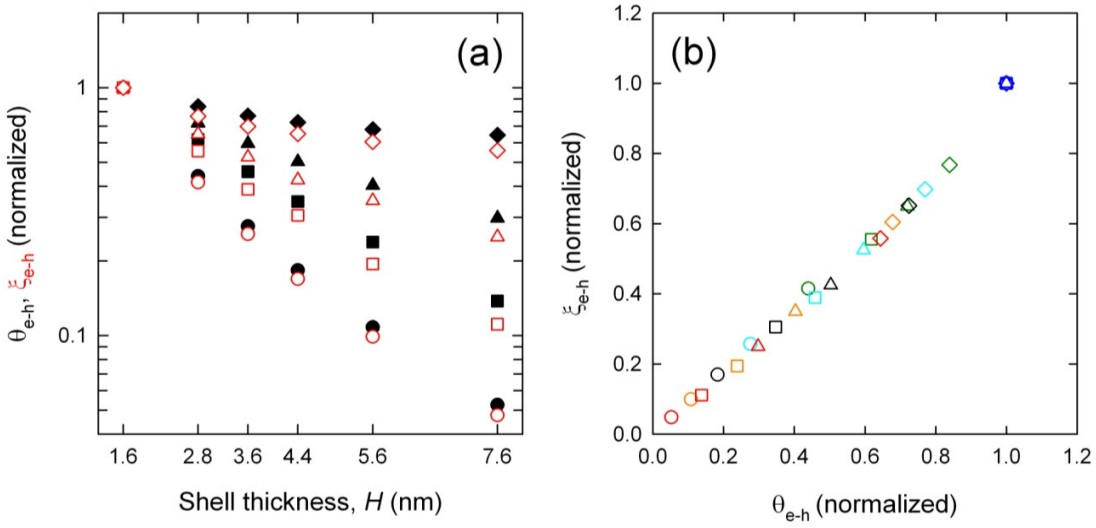


**Supplementary Figure S2. Theoretical analysis of the relationship between the electron-hole EI energy and the electron-hole overlap integral** (a) The exchange interaction term ($\xi_{e\text{-}h}$, hollow red symbols) and the electron-hole overlap integral ($\theta_{e\text{-}h}$, solid black symbols) as a function of shell thickness calculated according to refs.[1] and [3], using different values for the conduction-band energy offset at the CdSe/CdS interface: $\Delta E_e = 0$ (circles), 0.1 eV (squares), 0.2 eV (triangles) and 0.32 eV (diamonds). (b) Direct correlation between calculated alues of $\xi_{e\text{-}h}$ and $\theta_{e\text{-}h}$ for CdSe/xCdS NCs ($x = 4$, blue; $x = 7$, green; $x = 9$, cyan; $x = 11$, black; $x = 14$, orange; and $x = 19$, red). Both $\theta_{e\text{-}h}$ and $\xi_{e\text{-}h}$ are normalized to the value for CdSe/4CdS ($H = 1.6$ nm).

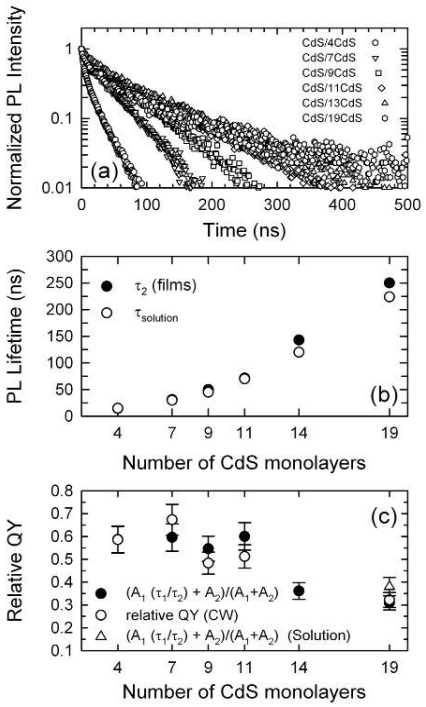


**Supplementary Figure S3. Time-resolved PL measurements for dilute solutions and solid films of CdSe/*x*CdS NCs: Validation of the method for estimations of radiative lifetimes from double-exponential fits.** (a) PL decay curves for diluted solutions of CdSe/CdS NCs with different shell thicknesses (excitation wavelength is 400 nm). (b) PL lifetimes extracted by single exponential fits of the decay curves for solutions (from 'a') in comparison with the lifetimes of the long-lived decay component measured for drop cast films. A remarkable agreement between the two sets of data confirms the validity of the approach in which the radiative lifetime of film samples is assumed to correspond to a slower time constant derived from double exponential fits. (c) Relative PL QYs measured under weak steady state excitation for the same solutions as in 'a' (open circles) compared to values extracted from the double-exponential fits of the decay curves for the drop-cast films using the expression $QY \propto [A_1(\tau_1/\tau_2)+A_2]/(A_1+A_2)$. Again, a very good agreement between the two data sets strongly supports the validiy of our approach for deriving the radiative lifetimes of film samples.

## Supplementary Table

| | CdSe | CdS |
|---|---|---|
| **Electron effective mass** | **0.13 *m0*** | **0.21 *m0*** |
| **Hole effective mass** | **0.45 *m0*** | **0.68 *m0*** |
| **Bandgap energy** | **1.75 eV** | **2.50 eV** |

**Supplementary Table S1.** Parameters of bulk CdSe and CdS used in the calculations shown in Supplementary Fig.S1 ($m_0$ is the electron rest mass).

## Supplementary Methods

Supplementary Figure S1a shows experimental values of PL peak spectral position and the room temperature decay times for core-shell CdSe/CdS NCs with various shell thicknesses ($R$ = 1.5 nm). A significant red-shift (~200 meV) of the 1S absorption band is observed upon growing one to 3 monolayers (ML) of CdS, as a result of progressively weaken quantum confinement in larger NCs. Most importantly, the 1S energy saturates for a ca. 4 ML shell, after which it remains constant independent on shell thickness (up to 19 CdS ML). This result, together with the data from Fig. 4a, indicate that in CdS/CdSe the effective exciton radius does not significantly increase with $H$ when the total NC radius exceeds ~4 nm.

While not significantly affecting the effective exciton size, the increasing leakage of the electron wavefunction into the shell region leads to an appreciable decrease in the electron-hole overlap integral with increasing $H$ as indicated by the measurements of PL dynamics. Specifically, as shown in Figs. 4d and Supplementary Fig S1a, the PL lifetime undergoes a progressive increase with increasing shell thickness, from $\tau$ = 15 ns for CdSe/4CdS to $\tau$=225 ns for CdSe/19CdS NCs.

The observed behaviors are consistent with results of theoretical calculations shown in Supplementary Figs. S1b and S1c. Good qualitative agreement is found for both the spectral position of the 1S transition and the PL lifetime (the latter is expected to be proportional to inverse overlap integral, $\theta^{-1}_{e\text{-}h}$, shown in Supplementary Fig. S1b by the dashed line). The calculations are based on the effective-mass model described in reference [38] in which we use the values of the electron and hole effective masses and the bang gap shown in Supplementary Table S1. Since the conduction-band energy offset at the CdSe-CdS interface ($\Delta E_e$) is not well established, in our calculations we have used two limiting values of 0 and 0.32 eV. The comparison of experimental and theoretical results indicates that whereas the experimental trends are qualitatively reproduced by calculations in both limits, a better quantitative agreement for the overlap integral is obtained assuming $\Delta E_e$ = 0 (Supplementary Fig. S1c). Thus, this analysis seems to indicate that the conduction band is essentially continuous at the CdSe/CdS interface (at least in the studied nanostructures).

The electron-hole overlap integral is defined as $\theta_{e-h} = \left| \int d^3 r \psi_e(r) \psi_h(r) \right|^2$, where $\psi_e$ and $\psi_h$ are electron and hole wavefunctions, respectively. The electron-hole EI energy is directly proportional to $\xi_{e-h} = \int d^3 r \left|\psi_e(r)\right|^2 \left|\psi_h(r)\right|^2$.[39] While an apparent similarity of the above two expressions is suggestive of a direct correlation between $\theta_{e\text{-}h}$ and $\xi_{e\text{-}h}$, it is not obvious that the relationship between $\xi_{e\text{-}h}$ and $\theta_{e\text{-}h}$ is described by a linear

dependence. To prove the existence of such a dependence, we have evaluated $\theta_{e\text{-}h}$ and $\xi_{e\text{-}h}$ as function of shell thickness using the model of ref.40. Further, since the conduction-band energy offset at the CdSe-CdS interface ($\Delta E_e$) is not well established, in our calculations we have varied it from 0 to 0.32 eV. The results of our calculations are displayed in Supplementary Figure S2.

As already discussed in the previous section, the electron-hole overlap integral decreases with $H$ for all values of $\Delta E_e$ used in the calculations (Supplementary Fig. S2a; solid symbols). Further, we observe that the rate of this decrease increases for smaller values of $\Delta E_e$. Interestingly, these behaviors are closely mimicked in the dependences of $\theta_{e\text{-}h}$ on $H$ for all conduction-band energy offsets (Supplementary Fig. S2a; open symbols). The similarity in the evolutions of $\theta_{e\text{-}h}$ and $\xi_{e\text{-}h}$ with $H$ leads to almost perfectly linear dependence of $\xi_{e\text{-}h}$ on $\theta_{e\text{-}h}$ (Supplementary Fig. S2b), suggesting that in these hetero-NCs, $\xi_{e\text{-}h}$ can be presented as $\Delta_{DB} = \Delta_0 \theta_{e-h}$, where $\Delta_0$ is the EI splitting in the case where the electron-hole overlap is unity. Further, since this linear scaling is observed independent on the value of $\Delta E_e$, it implies that the direct proportionality between $\Delta_{DB}$ and $\theta_{e\text{-}h}$ is likely a general property of core-shell systems with a tunable electron-hole overlap integral.

Supplementary Figure S3a displays the PL decay curves for dilute hexane solutions of CdSe/CdS NCs with different thicknesses of the CdS shell. All decays follow a nearly pure single exponential dynamics. The PL lifetimes extracted from single exponential fits are shown in Supplementary Fig. S3b by open circles. These results agree very well with the $\tau_2$-values obtained from the double exponential fits of the decay curves measured for film samples (Figs. 4 b, c). This confirms the validity of ascribing the long-lived portion of the decay curves of solid films to radiative recombination of excitons.

A further confirmation of the validity of this method is provided by the comparison of the relative PL quantum yields (QYs) of dilute NCs solutions (directly measured by referencing the time- and spectrally integrated emission intensity against the emission from standard dye, rhodamine-640) and the yields extracted from double-exponential fits of PL decay curves for solid films as described in the Methods section. Very good agreement is found between the data obtained by these two approaches, once again confirming that the long-lived portion of the decay curves is in fact due to radiative recombination.

**Supplementary References**


38 García-Santamaría, F. *et al.* Suppressed Auger Recombination in "Giant" Nanocrystals Boosts Optical Gain Performance. *Nano Lett.* **9**, 3482-3488, (2009).

39 Romestain, R. & Fishman, G. Excitonic wavefunction, correlation energy, exchange energy, and oscillator strenght in a cubic quantum-dot. *Phys. Rev. B* **49**, 1774-1781, (1994).

40 Piryatinski, A., Ivanov, S. A., Tretiak, S. & Klimov, V. I. Effect of quantum and dielectric confinement on the exciton-exciton interaction energy in type II core/shell semiconductor nanocrystals. *Nano Lett.* **7**, 108-115, (2007).